



NUMERICAL ANALYSIS OF FULL-SCALE FIVE STORY REINFORCED CONCRETE BUILDINGS

Y. Kido⁽¹⁾, T.Obara ⁽²⁾, S.Kono ⁽³⁾, T.Mukai ⁽⁴⁾, D.Mukai ⁽⁵⁾

⁽¹⁾ Graduate student, Tokyo Institute of Technology, Japan, yuki.kido1996@gmail.com

⁽²⁾ Assistant professor, Institute of Innovative Research, Tokyo Institute of Technology, Japan, obara.t.ac@m.titech.ac.jp

⁽³⁾ Professor, Institute of Innovative Research, Tokyo Institute of Technology, Japan, kono.s.ae@m.titech.ac.jp

⁽⁴⁾ Senior research engineer, Building Research Institute, Japan, t_mukai@kenken.go.jp

⁽⁵⁾ Associate Professor, Dept. of Civil and Architectural Engineering, University of Wyoming, dmukai@uwyo.edu

Abstract

Life safety was the major and perhaps the only concern in building structures in the earthquake engineering community a few decades ago. However, the 1994 Northridge earthquake and 1995 Kobe Earthquake revealed that the general public does not share the same vision with earthquake the engineering society. Urban earthquakes of the last twenty years have made it clear that earthquake resistant design needs to be performed to a higher standard, that is, damage of structures should be limited so that structures should keep their original functions after earthquakes. The 2004 AIJ guidelines for performance evaluation of earthquake resistant reinforced concrete buildings (draft) evaluates four limit states, Serviceability, Reparability I and II, and Safety limit states, by defining limiting values for residual deformation, residual crack width and strain condition of materials. In 2014 and 2015, two real scale five-story reinforced concrete buildings with or without structural gaps around non-structural walls, were tested at the Building Research Institute (BRI) in order to evaluate damage of beams, columns and walls. The flexural behavior was dominant in both specimens, therefore most cracks were governed by flexure and the number of shear crack was limited. In these tests, the number and length of cracks were measured as additional factors to define limit states of members. This paper describes a numerical method to evaluate damage of buildings in terms of crack width by using a fiber model.

This numerical model for buildings consists of fiber elements for flexural behavior and shear springs for shear behavior. The model reproduced base shear force – roof level drift angle relation and residual deformation with good accuracy. In order to evaluate the limit state of members, the strain condition of concrete and longitudinal reinforcement obtained from the model analysis was compared to experimental results. Also, the maximum residual flexural crack width was simulated using strain level from the fiber model. Using these results, the drift angle at each limit state was simulated with good accuracy. The numerical simulation was also conducted to evaluate detailed damage such as length and number of cracks. A threshold for each limit state for length and number of cracks is proposed based on the numerical results to determine the seismic performance of buildings for various earthquakes. The information will also be helpful to evaluate cost of repair after earthquake damage.

Keywords: Crack evaluation, RC Building analysis, Damage evaluation, Fiber model, Resilient buildings



1 Introduction

In the 2011 Pacific coast of Tohoku Earthquake, there are many cases[1] where it was difficult to continue using in accordance with reinforced concrete structures due to damage such as cracks in spite of the building being designed standards for earthquake resistant design developed 1981 in Japan[2]. The seismic performance required by the 1981 code is that no repair is necessary after a small or medium-sized earthquake, and that a large earthquake does not cause collapse and human lives are protected. In other words, immediate occupancy performance of the building after a large earthquake is not required by the 1981 standard. However there has been a growing demand for buildings to be capable of continuous use immediately after experiencing a large-scale earthquake disaster such as the Pacific coast of Tohoku Earthquake.

Therefore, the study about improving continuous use after an earthquake was conducted by the Ministry of Land Infrastructure, Transport and Tourism's comprehensive technology development project of "Development of technology to continue functioning at a disaster-base building". The two full-scale five-story reinforced concrete specimens in 2014 and 2015 (hereafter referred to as the 2014 and 2015 specimens) were subjected to static cyclic loading tests. In this study, wing walls, hanging walls, and spandrel walls, which had been treated as non-structural walls in conventional design methods, were treated as structural walls to reduce the response displacement of buildings to seismic forces and ensure continuous usability as much as possible.

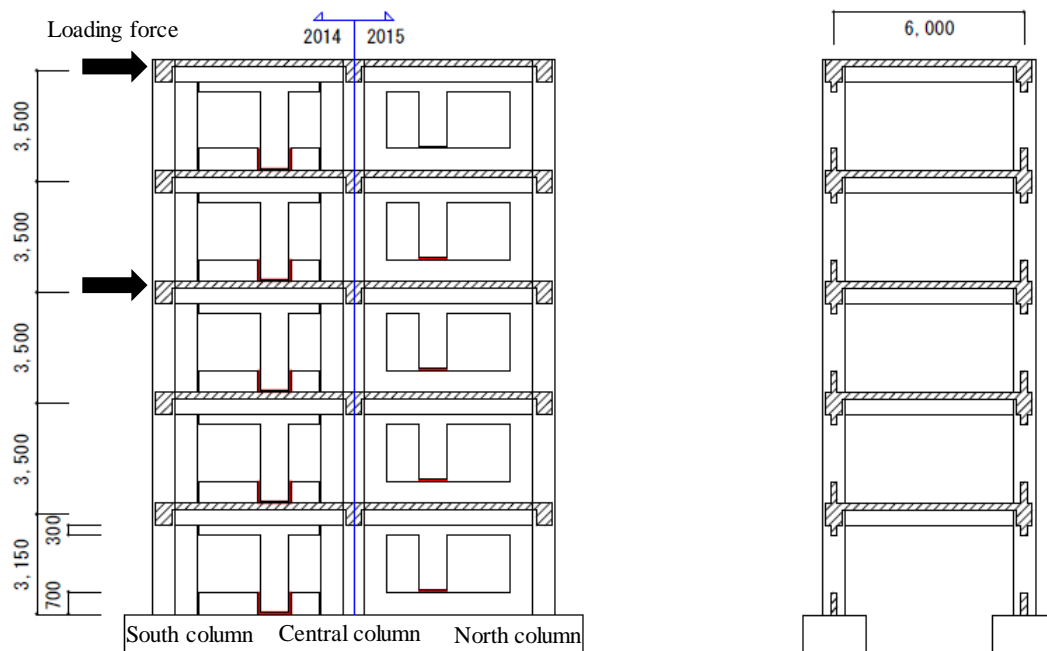
Mukai and colleagues studied a modeling method for the 2014 and 2015 specimens that can evaluate the behavior of the entire building using an end-spring model with the rigid region length and the effective width of the slab as the main analysis variables[3]. It was found that the backbone curve of the load-drift angle relationship of the whole building can be sufficiently reproduced by considering the appropriate rigid area length and the effective width of the slab. However the information such as residual deformation and energy consumption are urgently necessary to construct a cyclic model or a calculation equation that can evaluate continuous usability evaluation. In this study, a cyclic nonlinear fiber analysis model for the 2014 and 2015 specimens was constructed and the structural performance of the building including the residual drift angle and energy dissipation was evaluated.

2 Analysis model

2.1 Outline of the experiment and loading

The specimens are a full-scale five-story reinforced concrete frame shown in Figure 1 with two spans in the ridge direction (load plane direction) and one span in the span direction (transverse to the load plane). The floor height is 3.5m, the building height is 17.5m, and the span length is 6m in both the ridge direction and the span direction. The column section is 700 mm × 700 mm, the beam section is 500 × 700 mm, and the slab and wall thickness are 200 mm. In the 2014 test specimen, gaps were provided around the pier wall, hanging wall, and spandrel wall. In the 2015 test specimen, gaps were provided only at the pier wall base. As shown in Fig. 1, both specimens are conducted with cyclic loading so that the lateral force is 1: 2 on the roof and the 4th floor. Loading is displacement-controlled with the following target angles: $R_r = \pm 0.0625\%$, $\pm 0.125\%$ once, and thereafter $R_r = \pm 0.25\%$, $\pm 0.50\%$, $\pm 1.0\%$, $\pm 1.5\%$ (2014 specimen only), $\pm 2.0\%$ up to two cycles per drift. The drift angle R is obtained by dividing the lateral displacement of the roof by the total height of the building.

According to the experimental results, the 2014 test specimen showed that the waist wall and the pier wall, separated by a gap, contact each other at around $R = 1.35\%$, and the lateral capacity increased. The maximum base shear in the experiment was about 4400kN at $R = 1.0\%$ and the cracking at the contact point in the pier wall was significant. In the 2015 test specimen, the end of the wall of one to the first three floors collapsed typically near a drift angle of 1.0%, and the strength of the frame decreased. The edge of the waist wall and the pier wall buckled and the cover concrete spilled off at the corner of the opening. The maximum base shear was about 8000kN near $R = 0.5\%$. The detail is shown in [4].



(a) The frontal figure

(b) The lateral figure

(c) The plane figure

Fig.1 Plane view and side view of 2014/2015 specimen

2.2 Outline of analysis

The program used for this analysis is the elasto-plastic analysis program SNAP[5]. Figure 2 shows the modeled area around the wall. In the 2014 test specimen, gaps were provided around the pier wall, hanging wall, and spandrel wall, so they were not modeled in this analysis. Similarly the 2015 specimen did not model pier wall because it too was isolated by a gap.

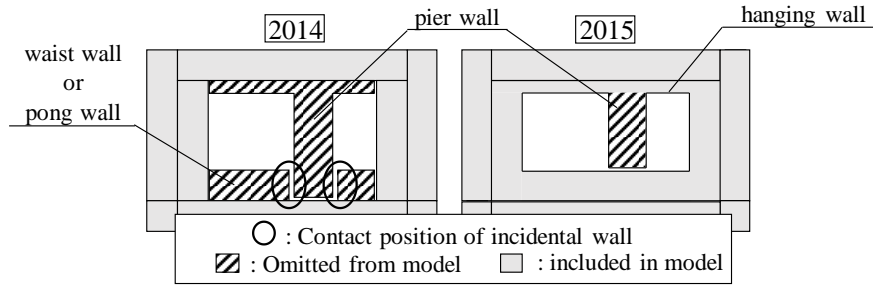


Fig.2 Modeled area around the wall

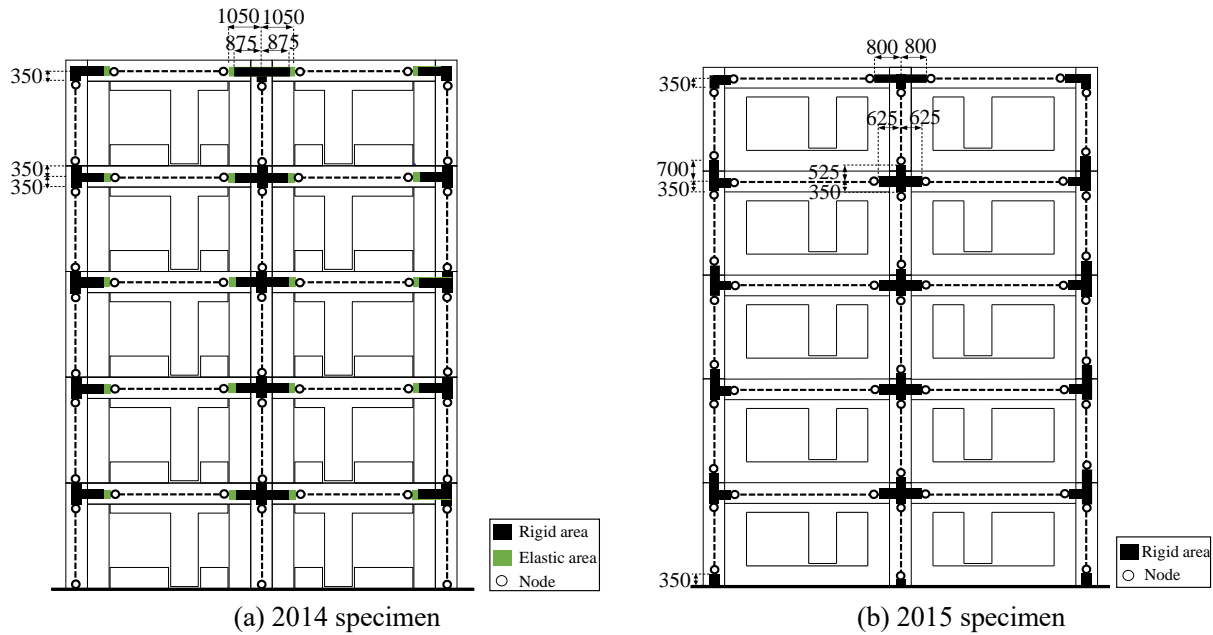


Fig.3 The set rigid area length of the member

The models for the frame (Figure 3) are made of rigid elements (black), elastic elements (green), and inelastic elements (dashed). The rigid elements have no deformation, the elastic elements have elastic deformations, and the inelastic elements have elastic and plastic deformations. According to [6], the rigid area length was set to be $D/4$ from the face of the column-beam joint, where D is the depth of the column plus wall. However, the spandrel wall and hanging wall in the 2014 test specimen were not included in the beam because they were insulated from the frame by gaps. When the rigid region length does not exceed the column-beam face interface, the column-beam face interface was defined as the rigid region end. The elastic region, the range from the end of the rigid region to the wing wall face, was used for the 2014 test specimen, and was not used for the 2015 test specimen. The bottom of the foundation level were assigned with fixed boundary condition.

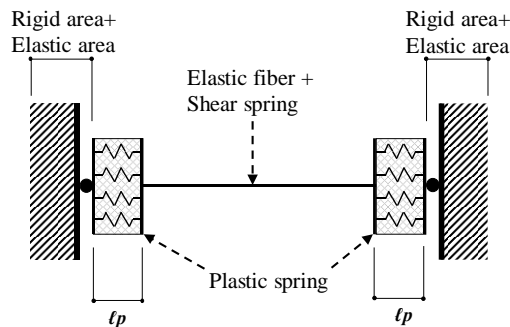


Fig.4 Inelastic elements

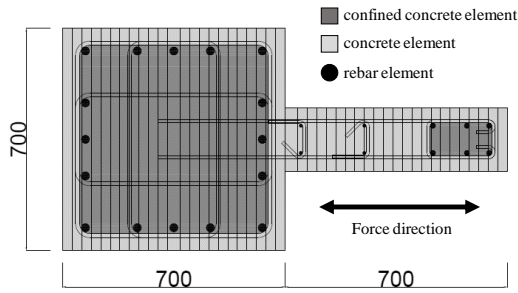
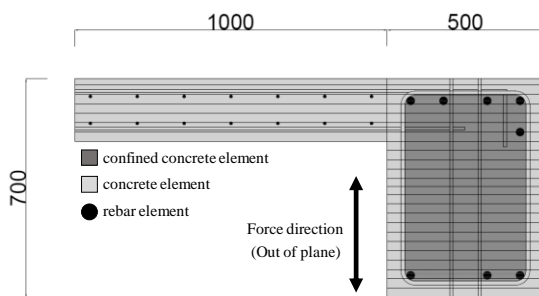
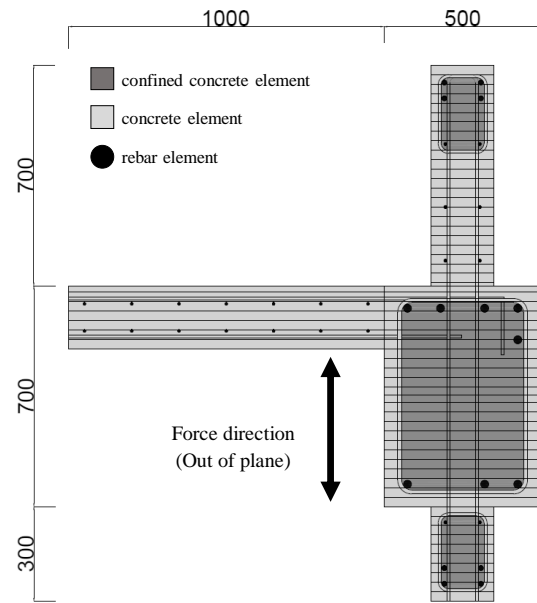


Fig.5 Sectional element division of column with wing wall of 2014/2015 specimen



(a) 2014 specimen



(b) 2015 specimen

Fig.6 Sectional element division of beam with wing wall of 2014/2015 specimen

The inelastic elements are made of shear and multi-spring sub-elements (Figure 4). Figure 4 shows a conceptual multi-spring model with length lp on both ends of the in elastic element connected with an elastic shear spring. The shear spring models the shear deformations which were elastic. The cross-sections of the actual multi-spring models are shown in Figure 5 and 6. All cross sections use confined concrete, unconfined concrete, and reinforcing steel elements. Due to symmetry, only half of the horizontal elements were modeled. Instead of modeling the slabs to their midspan, only their cooperating width of 1m [7] was modeled.

2.3 Material property of MS model

Figure 7 shows the stress-strain relationship for concrete and steel reinforcement used in the model. In the stress-strain relationship of concrete, the ascending leg till the maximum compressive strength was expressed by Hoshikuma's model[8], and the decrease in stress after maximum compressive strength was expressed by a straight line. For the confined core concrete, considering the restraining effect of the lateral reinforcing bars, the strain at maximum compressive strength $\epsilon_{cf,0}$ of the restrained concrete is calculated using equations (1) and (2) of the Son-Sakino model[9]. The maximum compressive strength F_{cf} was calculated from equation (3).

$$\epsilon_{cf,0}/\epsilon_0 = 1 + 4.7(K - 1) \quad (K \leq 1.5) \quad (1)$$

$$\epsilon_{cf,0}/\epsilon_0 = 3.35 + 20(K - 1.5) \quad (K > 1.5) \quad (2)$$

Where, $\epsilon_{cf,0}$: strain at the time of compressive strength of confined concrete,

ϵ_0 : Strain at compressive strength of unconfined concrete,

K : A coefficient representing the rate of increase in compressive strength of constrained concrete relative to unconfined concrete, according to equation (3).

$$K = F_{cf}/F_0 = 1 + \kappa p_b \sigma_{sy}/F_0 \quad (3)$$

Where, F_{cf} : compressive strength of confined concrete,



F_0 : Compressive strength of unconfined concrete,

κ : Quantitative coefficient of cross section subjected to compressive force,

p_b : Volume ratio of lateral reinforcement,

σ_{sy} : Yield strength of lateral reinforcement.

The ultimate limit strain $\mu\epsilon_0$ was 1.0% for unconfined concrete, and the ultimate strain for confined concrete was calculated using the equation proposed by Priestley et al[10]. Tensile strength f_t was calculated using equation (4).

$$f_t = 0.33\sqrt{f'_c} \quad (4)$$

Where f'_c : Concrete compressive strength in Mpa

f_t : Tensile strength in Mpa

The stress-strain relationship of the reinforcement was modeled assuming the stiffness after yielding to be 0.001 times the initial stiffness.

A modified Ramberg-Osgood model was used for modeling cyclic behavior.

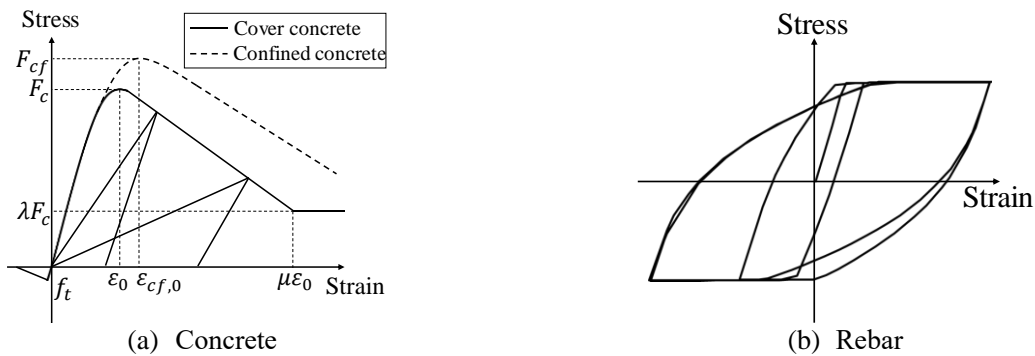


Fig.7 Stress-strain curve

3 Analysis result

3.1 Base shear(Q)-Drift angle(R) relationship

Figure 8 shows the base shear (Q) –drift angle (R) relationship of each specimen. The base shear was the sum of the lateral forces of four floors and the roof, and drift angle was the value obtained by dividing the horizontal displacement of the roof by the height of the roof.

In the test of the 2014 test specimen, the waist and pier walls came into contact before a drift angle of $R = 1.5\%$ and the lateral capacity increased, so this study is limited to a drift angle $R = 1.0\%$ before this contact occurred.

The analysis was able to accurately reproduce the experiment up to a drift angle of $R = 1.0\%$. As shown in Table 1, the maximum base shear was within 6.0% of experimental values, and the drift angle at the maximum base shear was almost equal to experimental values. In addition, if the pier wall contact did not happen at drift angles greater or equal to $R=1.35\%$, it is assumed that the maximum base shear would not increase as in the analysis. The base shear of the analysis was slightly larger than that of the experiment up to $R = 0.5\%$, this was due to the fact that effective width of the slab set in the analysis was larger than the actual one when the drift angle was small.

In the 2015 test specimen, the hysteresis characteristics including the unloading stiffness were reproduced with the same high accuracy as the 2014 test specimen. However, up to $R = 0.5\%$, the base shear of the analysis



was slightly higher than the experimental value, similar to the 2014 specimen. The maximum base shear obtained from the analysis had only a 5.0% less than the value obtained from the experiment. However, the typical drift angle at the maximum base shear occurred during the $R = 0.5\%$ in the experiment and $R = 1.0\%$ in the analysis. Because the maximum base shear point occurred in different cycles in the analysis and experiment, the corresponding maximum drift angles differ by 48%. Regarding the stiffness and base shear at small drift angles it is necessary to examine the validity of modeling the hanging wall, waist wall, and pier wall with gaps in addition to the effective width of the slab. Overall, it was found that the experimental results could be reproduced with good accuracy by the model.

Table 1 Maximum base shear and drift angle ratios for each specimen

specimen	Q(kN)		R(%)	
	[Exp/analysis]		[Exp/Analysis]	
	Positive	Negative	Positive	Negative
2014	1.06	1.07	1.00	1.00
2015	1.05	1.02	1.48	0.96

Q:Maximum base shear, R: Drift angle at maximum base shear

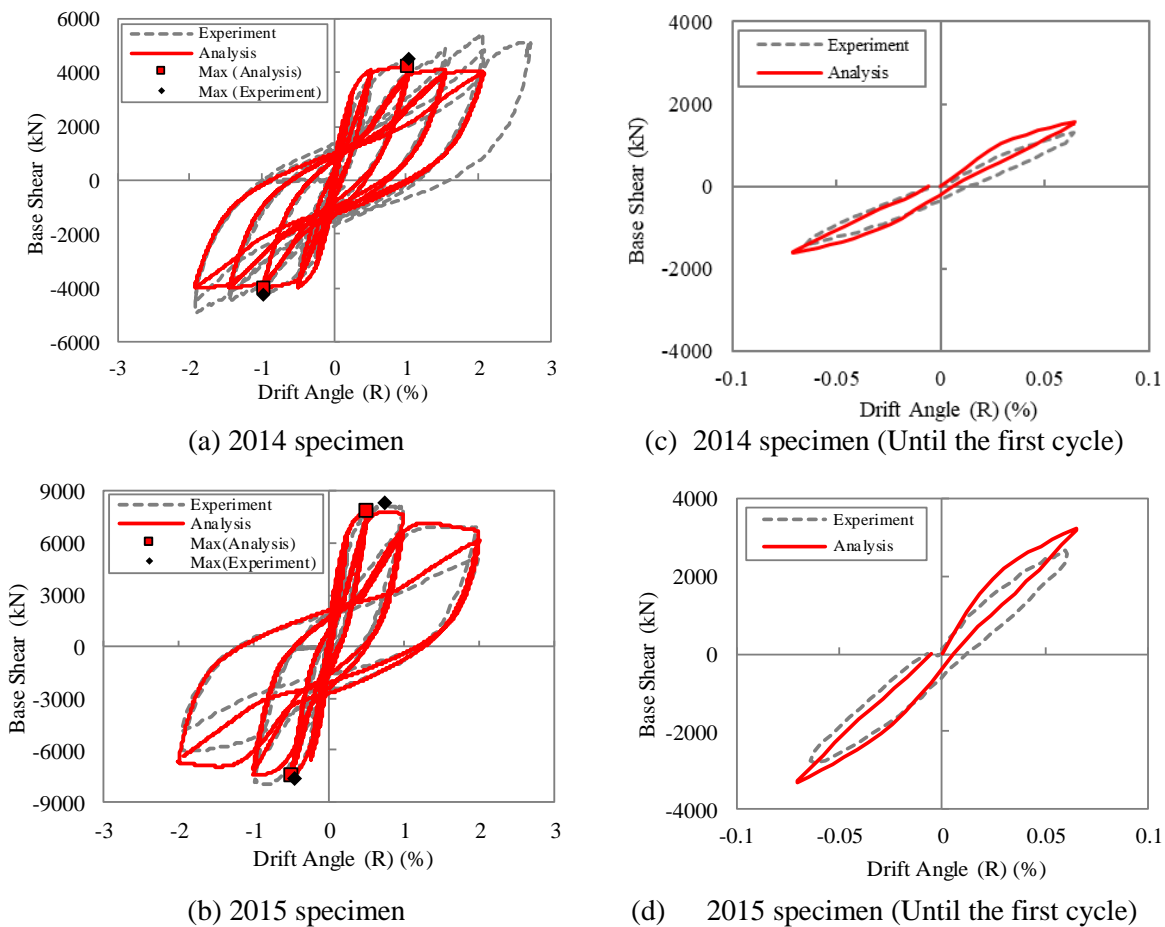


Fig.8 Experiment and analysis comparison in Q-R relationship

3.2 Plastic hinge formation



Figure 9 shows a comparison of plastic hinge distribution between the analysis and experiment. The plastic hinge formation position in the experiment, was determined by the procedure described in [3], plastic hinge formed at a drift values of $R=0.5\%$ are indicated by white circles and those formed at a drift of 1.0% are indicated by red circles. In the analysis, it was assumed that the plastic hinge was formed when the longitudinal of the member section reached the yield strain.

The model captured the tendency of plastic hinges forming at beam ends in the 2014 experiment, and was able to almost reproduce the formation of all the plastic hinges at the correct drift angles. In the case of the beams of R and 4 levels, the hinge is formed at later cycles than in the experiment. In the 2015 test specimen, the partial yielding specimen, the damage was limited to the first three floors in the experiment. The model generally reproduces this behavior.

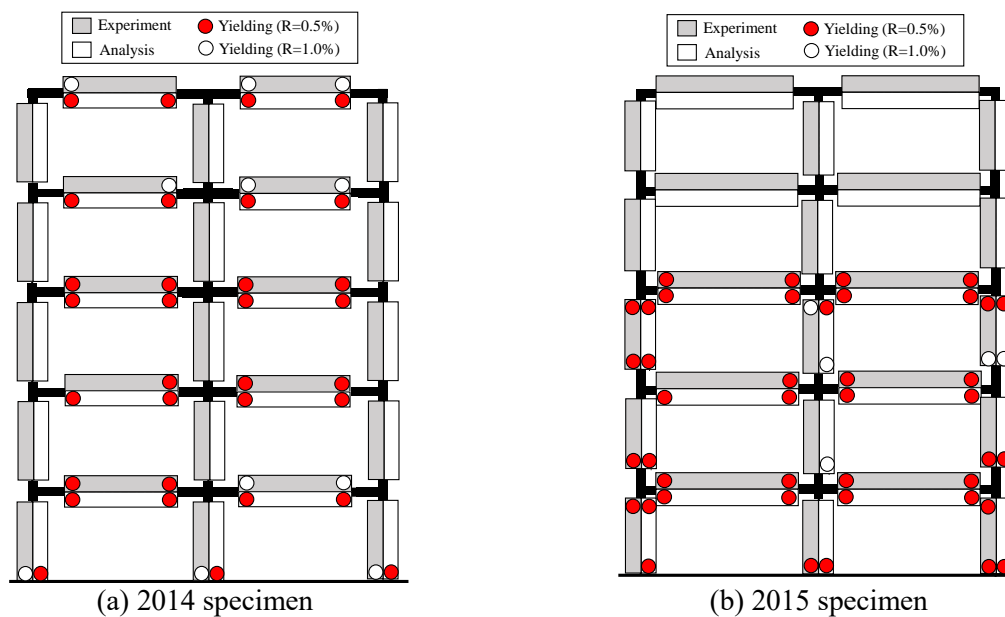


Fig.9 Experiment and analysis comparison in plastic hinge distribution

3.3 Residual drift angle

Figure 10 shows the relationship between the residual drift angle and the drift angle of each specimen up to the drift angle of $R = 2.0\%$. The residual drift angle was defined as the drift value (R) occurring at 0kN base shear (Q) -drift angle (R) relationship shown in Fig. 8, and was calculated from the average value of the second cycle positive load side and the negative load side drifts.

The model was able to reproduce the experimental value of 2014 specimen with high accuracy up to $R = 1.0\%$. The experimental values after $R = 1.0\%$ are considered to have increased residual drift angle due to the damage caused by the contact between the waist wall and pier wall.

The model could replicate the experimental value of 2015 specimen with high accuracy up to $R = 2.0\%$. The experimental value after $R = 0.5\%$ became larger than that of the 2014 specimen, and the analysis could reproduce this behavior.

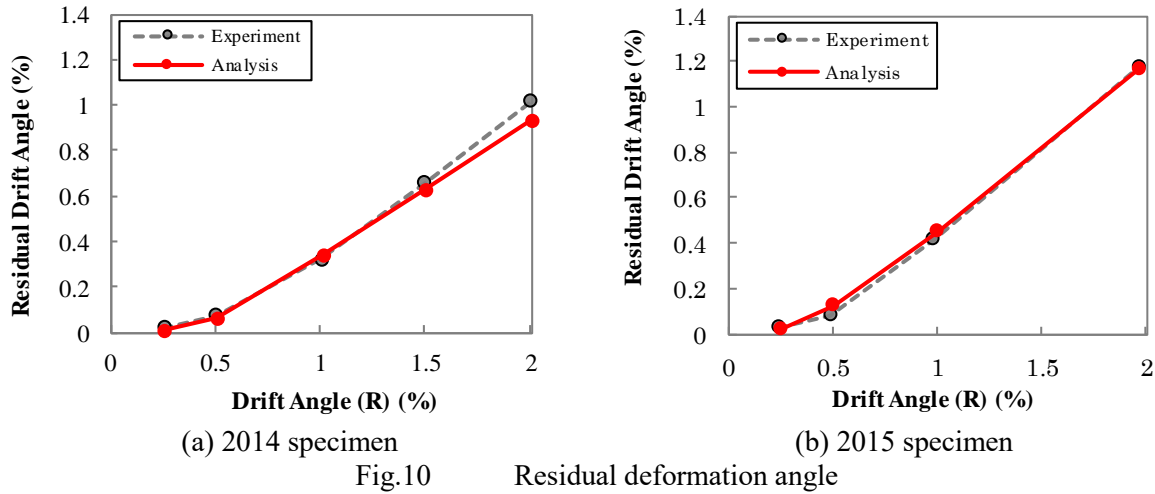


Fig.10 Residual deformation angle

3.4 Energy Dissipation

Figure 11 shows the relationship between energy dissipation (h_{eq}) and drift angle. The energy dissipation was calculated using the hysteresis loop of the second cycle for each drift angle for both analysis and experiment, in accordance with [11].

The 2014 specimens model was able to closely reproduce the experimental values up to $R = 1.0\%$. Although the analysis values are slightly smaller than the experimental values, this is conservative. The values up to $R = 2.0\%$ are shown for reference, which shows that if the waist wall does not contact the pier wall, about $h_{eq} = 15\%$ can be expected when $R = 2.0\%$.

In the 2015 specimen, the experimental values are reproduced up to $R = 2.0\%$ as in the 2014 specimen. In the experiment, after $R = 0.5\%$, the energy dissipation obtained was larger than that of the 2014 specimen. The analysis could reproduce this tendency.

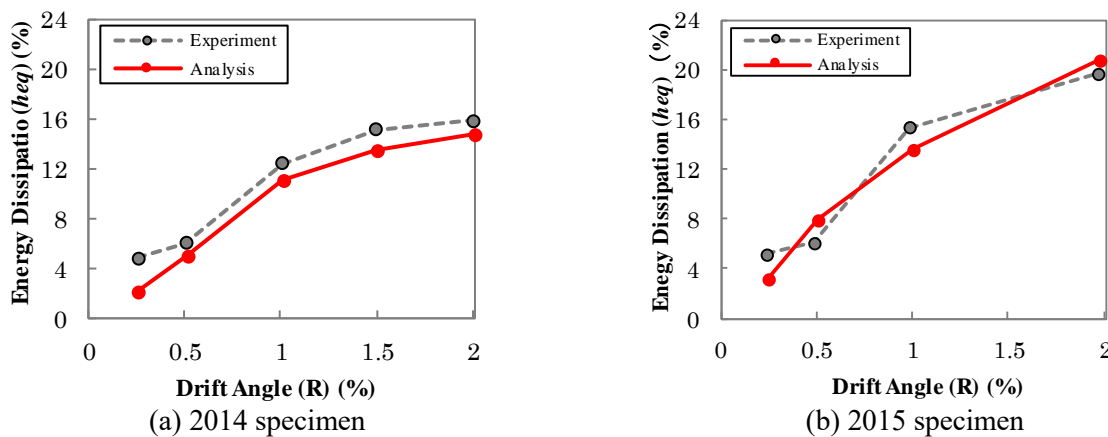


Fig.11 Energy dissipation



4 Conclusions

An analytical model of a full-scale 5-story RC building was created to evaluate the continuous use of building after an earthquake, and the relationship between base shear and drift angle, residual deformation angle, energy dissipation and plastic hinge distribution.

Models for full-scale specimens tested in 2014 and 2015 both can accurately reproduce the Q-R relationship, plastic hinge formation status, residual deformation angle, and energy dissipation with high accuracy up to a drift angle of $R=2.0\%$.

For the future research, the strain and neutral axis location of members will be evaluated using this analysis model, and a damage evaluation method based on the amount of cracking will be proposed.

5 Acknowledgements

This work was supported financially by JSPS through a Grant-in-Aid program (PI: S. Kono). We are thankful to Collaborative Research Project (Materials and Structures Laboratory), and the World Research Hub Initiative (Institute of Innovative Research), at Tokyo Institute of Technology for their generous support of this research.

6 References

- [1] Ministry of Construction (1980): Enforcement Ordinance of Construction Standard Law
- [2] National Institute for Land and Infrastructure Management Ministry of Land/Infrastructure/Transport and Tourism, Japan; Building Research Institute Incorporated Administrative Institution, Japan, :“Report on Field Surveys and Subsequent Investigations of Building Damage Following the 2011 off the Pacific coast of Tohoku earthquake,” TECHNICAL NOTE National Institute for Land and Infrastructure Management No.64 /Building Research data No.136, 2012.3.
- [3] Toshikazu K, Yuma K, Hideyuki K, Susumu K, Masaki M, Masanori T, Hidekazu W, Masanobu S: Static nonlinear analysis of a full scale five story reinforced concrete building, Summaries of technical papers of annual meeting Architectural Institute of Japan, pp.539-542, 2018,9
- [4] Toshikazu K, Tomohisa M, Hiroshi F, Hiroto K, Haruhiko S, Masaomi T, Koichi K: A full scale static loading test on five story reinforced concrete building utilizing columns with wing walls, J. struct. Constr. Eng., Summaries of technical papers of annual meeting Architectural Institute of Japan. Vol81 No.720, p313-322, 2016 ,2
- [5] Structure System Corp. (2019): Elastic and plastic analytic program of Three-dimensional frame, SNAP Ver.7 [In Japanese]
- [6] Yuma K, Tomohisa M, Hideyuki K: Investigation of modeling method for walled frames based on static nonlinear analysis Proceedings of the Japan Concrete Institute, pp.79-84, 2017, 8
- [7] Architectural Institute of Japan (2010): Guidelines for performance evaluation of earthquake resistant reinforced concrete buildings [In Japanese]
- [8] Hoshikuma J, Kawashima K and Nagaya, K: A stress-strain model for reinforced concrete columns confined by lateral reinforcement, Japan Society of Civil Engineering, pp. 1-11, 1995, 8 [In Japanese]
- [9] Proceedings of the Japan Concrete Institute (1996): Concrete Handbook 2nd Edition, pp249~250 [In Japanese]



- [10] B.D. Scott, R. Park, M.J.N. Priestley: Stress-strain behavior of concrete confined by overlapping hoops at low and high strain rates, ACI Journal, pp. 13-27, 1982
- [11] Akenori S. (2014): Dynamic Analysis of Earthquake Resistant Structures, Morikita Publishing [In Japanese]